Numerical Solution of Nonlinear Exterior Wave Problems Using Local Absorbing Boundary Conditions

Igor Patlashenko,[1] **Dan Givoli**[2]

Abstract: The method of Absorbing Boundary Conditions (ABCs) is considered for the numerical solution of a class of nonlinear exterior wave scattering problems. Recently, a scheme based on the exact nonlocal Dirichlet-to-Neumann (DtN) ABC has been proposed for such problems. Although this method is very accurate, it is also highly expensive computationally. In this paper, the nonlocal ABC is replaced by a low-order local ABC, which is obtained by localizing the DtN condition in a certain "optimal" way. The performance of the new local scheme is compared to that of the nonlocal scheme via numerical experiments in two dimensions.

keyword: Exterior problems, Absorbing boundary condition, Unbounded domain, Dirichlet-to-Neumann (DtN), Finite elements.

1 Introduction

One class of numerical methods to solve exterior wave scattering or radiation problems is based on Absorbing (or Artificial) Boundary Conditions (ABCs). In this method, an artificial boundary B is introduced around the scatterer, a special boundary condition is imposed on B, and the problem is then solved numerically in the finite domain Ω bounded by B and the scatterer's surface Γ. The method of ABCs is commonly used for the solution of problems in unbounded domains, side by side with other methods such as Boundary Elements, Infinite Elements and Absorbing Layers. For a review on the subject, see Givoli (1991)–Tsynkov (1998).

The setup for the method of ABCs is illustrated in Fig. 1. The artificial boundary B is chosen to be a circle (in two dimensions) or a sphere (in three dimensions), although some ABC schemes are able to accommodate artificial boundaries of more general shapes. The domain exterior to B, which is eliminated in this method, is denoted D. The problem in Ω is usually solved by the finite element method.

Linear exterior wave problems have been dealt with quite a lot using the method of ABCs. On the other hand, a similar treatment of *nonlinear* wave problems is much more problematic, since most ABCs were not directly designed to account for nonlinearities in the exterior domain. As an important example, the family of Bayliss-Turkel ABCs (Bayliss and Turkel (1980)) is based on an exact solution of the governing equations in the far field, and such an exact solution is non-available with nonlinearities which extend to infinity. The method of ABCs was applied to nonlinear flow problems in Ferm and Gustafsson (1982)–Verhoff and Stookesberry (1992) for the solution of the Euler flow equations in an infinite domain, and in Hagstrom (1991)–Danowitz, Abarbanel and Turkel (1995) for the Navier-Stokes equations.

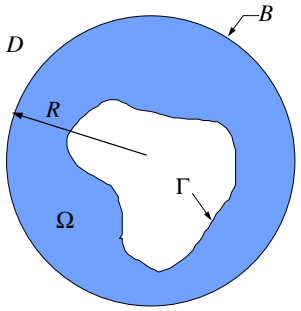

Figure 1 : Setup for the method of ABCs.

Recently (Givoli and Patlashenko (1998)), we devised a new ABC-type method for *nonlinear* exterior wave problems. This method makes a sequential use of the Dirichlet-to-Neumann (DtN) boundary condition. The DtN condition is a *nonlocal* ABC which is *exact* when applied to linear elliptic problems, such as the Helmholtz equation. See Givoli (1999) for recent review articles on the subject. The method proposed in Givoli and Patlashenko (1998) for a nonlinear hyperbolic wave problem is based on reducing the original problem into a sequence of linear elliptic problems, and applying the DtN condition on B for each problem.

This method yields very accurate results, but it also requires a large computational effort. The computationally intensive part of the scheme is the repeated calculation associated with the nonlocal DtN boundary condition. In addition, the nonlocality of the DtN condition generates a small full block in the finite element stiffness matrix, thus reducing the sparseness of the matrix. This does not introduce any difficulties if an iterative linear solver is used (see Givoli (1999); Malhorta and Pinsky (1996)), but with a direct solver this is commonly regarded as a deficiency.

Therefore, it is desirable to replace the nonlocal DtN condition

[1] Hummingbird Communications, Toronto, Canada
[2] Department of Aerospace Engineering,Technion, Israel

by a much simpler *local* ABC. Of course, this would result in some loss of accuracy, or, looked at differently, this would require to set the artificial boundary B further away from the scatterer in order to maintain the same level of accuracy. However, the use of a simple local ABC is very appealing, since it may be coded easily into standard finite element software, and it does not entail any compromise in the sparseness of the global stiffness matrix. Also, we shall see that if the local ABC used on B is properly designed, the errors it generates are not much larger than those generated by the DtN condition. On the other hand, as was shown in Givoli and Patlashenko (1998), the use of a overly "naive" local ABC like the Sommerfeld condition may lead to totally erroneous numerical results.

In this paper, we use the general scheme proposed in Givoli and Patlashenko (1998) for the solution of nonlinear exterior wave problems, but we replace the nonlocal DtN condition on B by one of the "optimal" local ABCs devised in Givoli and Patlashenko (1998) (in the context of linear elliptic problems). These ABCs are obtained by localizing the DtN condition in a way which aims at making the "distance" between the new local ABC and the nonlocal DtN condition as small as possible, in the L_2 sense. The theoretical properties of the optimal local ABCs have been investigated in Sidi and Givoli (2000). Their use has recently been extended to time-dependent waves in Patlashenko and Givoli (2000), still in the linear regime. Here we show that their use for *nonlinear time-dependent* waves results in a numerical scheme which is almost as accurate as the original scheme proposed in Givoli and Patlashenko (1998) and significantly more efficient.

Nonlinear waves in unbounded media are encountered in a variety of applications Whitham (1974)–Strauss (1989). The nonlinearity may originate from the material constitutive relations, from the large amplitude of the motion, or from the presence of a free boundary. In this paper we develop the numerical framework in the context of a model problem, governed by the two-dimensional nonlinear Klein-Gordon equation (Strauss (1989)). This equation has important applications in quantum physics. It also describes waves in a membrane lying on a nonlinear elastic foundation. However, more importantly, it serves as a relatively simple model for nonlinear wave problems which helps to bring to light most of the computational issues involved.

Following is the outline of the paper. In Section 2 we state the model problem under consideration, and discretize it in time, using the two-parameter implicit Newmark family of time integration schemes. This leads to a time-stepping scheme, where a nonlinear exterior elliptic problem has to be solved in each time step. In Section 3 we introduce an artificial boundary B which bounds the computational domain Ω. Then we apply a simple-iteration procedure to repeatedly linearize the elliptic problem in the infinite domain D outside B. To complete the scheme we apply an optimal local ABC on B. In Section 4 we discuss the finite element solution procedure and some computational aspects of the scheme. In Section 5 we demonstrate the performance of the scheme via numerical experiments. We conclude with some remarks in Section 6.

2 Problem Statement and Time Discretization

We consider the two-dimensional infinite domain R outside an obstacle with boundary Γ. In R, the nonlinear version of the Klein-Gordon equation governs (Strauss (1989)):

$$\ddot{u} - c^2\nabla^2 u = f(u) \tag{1}$$

Here $u(x,t)$ is the unknown wave function, x is the position vector in space, t is time, c is a given constant wave speed, and $f(u)$ is a given nonlinear function. A superposed dot denotes differentiation with respect to t.

The obstacle boundary Γ is divided into two parts: $\Gamma = \Gamma_g \cup \Gamma_h$. On Γ_g a Dirichlet condition is given, whereas on Γ_h a Neumann condition is given:

$$u = g \quad \text{on} \quad \Gamma_g \tag{2}$$

$$\frac{\partial u}{\partial \nu} = h \quad \text{on} \quad \Gamma_h \tag{3}$$

Here $\partial/\partial\nu$ is the normal derivative on Γ_h, and g and h are given functions. Initial conditions are given for u and $\dot{u}$:

$$u(x,0) = u_0(x), \qquad \dot{u}(x,0) = v_0(x) \tag{4}$$

Here u_0 and v_0 are given functions with compact support. At infinity the solution is bounded.

The first step in the proposed numerical method is to *discretize the problem in time*. To fix ideas we choose the two-parameter Newmark family of time-integration schemes, although other algorithms can be considered as well. Let Δt be the (constant) time-step interval, and let t_n be the time after n time-steps. Also, let u_n, v_n and a_n be the approximations of u, $\dot{u}$ and $\ddot{u}$ at time t_n, and let $0 < \beta \leq 0.5$ and $0 \leq \gamma \leq 1$ be the two Newmark parameters which determine the stability and accuracy properties of the scheme. We are interested only in *implicit* schemes, and therefore we exclude the case $\beta = 0$. The Newmark method applied to equations (1)–(3) may be written in a predictor-corrector form, namely:

Prediction:

$$\tilde{u}_{n+1} = u_n + \Delta t\, v_n + \frac{(\Delta t)^2}{2}(1-2\beta)\, a_n \tag{5}$$

$$\tilde{v}_{n+1} = v_n + \Delta t(1-\gamma)\, a_n \tag{6}$$

Solution:

$$(1 - (\Delta t)^2\beta c^2\nabla^2)\; u_{n+1} = \tilde{u}_{n+1} + (\Delta t)^2\beta f(u_{n+1}) \tag{7}$$

$$u_{n+1} = g_{n+1} \quad \text{on} \quad \Gamma_g \tag{8}$$

$$\frac{\partial u_{n+1}}{\partial \nu} = h_{n+1} \quad \text{on} \quad \Gamma_h \tag{9}$$

$$u_{n+1} < \infty \quad \text{at infinity} \tag{10}$$

Correction:

$$a_{n+1} = \frac{1}{\beta(\Delta t)^2}(u_{n+1} - \tilde{u}_{n+1}) \tag{11}$$

$$v_{n+1} = \tilde{v}_{n+1} + \gamma \Delta t\, a_{n+1} \tag{12}$$

Thus, in addition to the updating performed in the prediction and correction phases, one has to solve in each time-step the elliptic problem (7)–(10) in the unbounded domain R.

To write (7) more concisely we define,

$$\alpha = (c\Delta t\sqrt{\beta})^{-1},\ \ \tilde{f}(u_{n+1}) = \alpha^2\left(\tilde{u}_{n+1} + (\Delta t)^2\beta f(u_{n+1})\right) \tag{13}$$

Then (7) becomes,

$$\nabla^2 u_{n+1} - \alpha^2 u_{n+1} + \tilde{f}(u_{n+1}) = 0 \tag{14}$$

3 Truncation, Linearization and Application of ABC

We now introduce a circular artificial boundary B of radius R which encloses the obstacle and bounds the computational domain Ω. The infinite domain outside B is denoted D, i.e., $D = R - \Omega$. See Fig. 1.

We employ a simple-iteration procedure to replace the nonlinear equation (14) in D by a sequence of linear equations. The solution u_{n+1} in iteration i is denoted $u_{n+1}^{(i)}$. Equation (14) is replaced by,

$$\nabla^2 u_{n+1}^{(i+1)} - \alpha^2 u_{n+1}^{(i+1)} = -\tilde{f}(u_{n+1}^{(i)}) \quad \text{in} \quad D \tag{15}$$

Since $u_{n+1}^{(i)}$ is known at the $i+1$ iteration, the function $\tilde{f}$ in (15) is just a given function of x, and thus (15) is a *linear* elliptic equation. Also, the boundedness condition (10) is written as

$$u_{n+1}^{(i+1)} < \infty \quad \text{at infinity} \tag{16}$$

Note that (15) replaces (14) only in the exterior domain D. In the computational domain Ω, the governing equation remains the nonlinear equation (14).

The next step is to solve the problem (15) and (16) in D *analytically* in order to obtain the exact nonlocal DtN boundary condition. In the remainder of this section we shall omit the index $(i+1)$ for brevity. We shall also use $\tilde{f}$ to mean $\tilde{f}(u_{n+1}^{(i)})$. Note that at the current iteration $\tilde{f}$ is a known function. By following Givoli (1992) (but slightly simplifying the expressions given there), we obtain at time-step $n+1$:

$$\begin{aligned} u_{n+1}(r,\theta) = {} & \frac{1}{\pi}{\sum_{m=0}^{\infty}}' \frac{K_m(\alpha r)}{K_m(\alpha R)} \int_0^{2\pi} \cos m(\theta-\theta')\ u_{n+1}(R,\theta')\, d\theta' \\ & + {\sum_{m=0}^{\infty}}' \int_R^{\infty} \xi G_m(r,\xi)\,(\tilde{f}^c_{n+1,m}(\xi)\cos m\theta \\ & + \tilde{f}^s_{n+1,m}(\xi)\sin m\theta)\, d\xi \end{aligned} \tag{17}$$

Here a prime after a sum indicates that a factor of 1/2 multiplies the term with $n = 0$. Also,

$$\begin{aligned} \tilde{f}^c_{n+1,m}(\xi) &= \frac{1}{\pi}\int_0^{2\pi} \cos m\theta\ \tilde{f}_{n+1}(\xi,\theta)\, d\theta \\ \tilde{f}^s_{n+1,m}(\xi) &= \frac{1}{\pi}\int_0^{2\pi} \sin m\theta\ \tilde{f}_{n+1}(\xi,\theta)\, d\theta \end{aligned} \tag{18}$$

are the Fourier coefficients of $\tilde{f}_{n+1}$, and $G_m(r,\xi)$ is the one-dimensional Green's function given by

$$G_m(r,\xi) = \begin{cases} \dfrac{K_m(\alpha\xi)}{K_m(\alpha R)}\left[I_m(\alpha r)K_m(\alpha R) - K_m(\alpha r)I_m(\alpha R)\right] & r \le \xi \\ \dfrac{K_m(\alpha r)}{K_m(\alpha R)}\left[I_m(\alpha\xi)K_m(\alpha R) - K_m(\alpha\xi)I_m(\alpha R)\right] & r \ge \xi \end{cases} \tag{19}$$

In (17) and (19), I_m and K_m are the modified Bessel functions of the first and second kind.

Differentiating both sides of (17) with respect to r and then setting $r = R$ yields, after some algebra,

$$\frac{\partial u_{n+1}}{\partial r} = -M\, u_{n+1} + H[\tilde{f}_{n+1}] \quad \text{on} \quad B \tag{20}$$

$$M\, u = {\sum_{m=0}^{M}}' \int_0^{2\pi} k_m(\theta-\theta')u(R,\theta')\, R\, d\theta' \tag{21}$$

$$k_m(\theta-\theta') = \frac{Z_m}{\pi R}\cos m(\theta-\theta') \tag{22}$$

$$Z_m = -\alpha\frac{K_m'(\alpha R)}{K_m(\alpha R)} \tag{23}$$

$$\begin{aligned} H[\tilde{f}](\theta) = {} & {\sum_{m=0}^{M}}' \frac{1}{RK_m(\alpha R)} \int_R^{\infty} \xi K_m(\alpha\xi)\,[\tilde{f}^c_m(\xi)\cos m\theta + \\ & \tilde{f}^s_m(\xi)\sin m\theta]\, d\xi \end{aligned} \tag{24}$$

Equation (20) is an exact DtN boundary condition on B. Note that in (21) and (24) we have truncated the infinite series after a finite number of terms, M. For more details see Givoli (1992).

The DtN condition (20) is nonlocal in space. We wish to approximate it by a *local* ABC. To this end, we shall use the methodology of optimal local ABCs devised in Givoli and Patlashenko (1998) for linear elliptic problems. This methodology relates to the homogeneous counterpart of (20), namely to the replacement of the integral operator M by a differential operator. The inhomogeneous term $H[\tilde{f}_{n+1}]$ in (20) remains unchanged, and is calculated by using (24).

In order to approximate the nonlocal operator M by an Nth-order *local* operator, we replace (20) by

$$\frac{\partial u_{n+1}}{\partial r} = -L_N u_{n+1} + H[\tilde{f}_{n+1}] \quad \text{on} \quad B\ , \tag{25}$$

where

$$(L_N u)(\theta) \equiv \frac{1}{R}\sum_{m=0}^{N} A_m \frac{\partial^{2m} u}{\partial\theta^{2m}}\ . \tag{26}$$

Here the A_m are constant coefficients. The functions u to which the operator L_N is applied are assumed to be represented by the truncated Fourier expansion

$$u = \sum_{j=0}^{M}{}' (u_j^c \cos j\theta + u_j^s \sin j\theta) \ . \tag{27}$$

Here, M is a chosen number of modes (the same number as in (24)), and $M \geq N$. Now we pose the following minimization problem: Find the coefficients A_m in the local ABC (25)–(26) such that $(M - L_N)u$ is minimized in the L_2 sense, for functions u of the form (27). The minimizers A_m depend on both N (the order of the derivatives used in the local ABC) and on M (the number of represented modes); thus, the procedure described here leads to a two-parameter (N, M) family of schemes.

To find the desired coefficients A_m, we apply both operators M and L to the function u given by (27), and estimate the difference $||(M - L_N)u||_0^2$, where $||\cdot||_0$ is the L_2 norm. This yields (see Givoli and Patlashenko (1998))

$$||(M - L_N)u||_0^2 \leq ||u||_0^2 \ ||\beta^N||^2 \ , \tag{28}$$

where the second norm on the right side is the Euclidian norm of the vector β^N, whose entries are given by

$$\beta_j^N = Z_j - \sum_{k=0}^{N} A_k (-1)^k j^{2k} \ . \tag{29}$$

Assuming that nothing is known about the exact solution (see Givoli and Patlashenko (1998) for an alternative case), we conclude from (28) that the minimization of $||(M - L_N)u||_0^2$ leads to the minimization of $||\beta^N||^2$. A necessary condition for a minimum is $\partial||\beta^N||^2/\partial A_l = 0$ for $l = 0, \ldots, N$. This gives the linear symmetric system of equations,

$$BA = P \ , \tag{30}$$

where

$$P_l = \sum_{j=0}^{M}{}' Z_j (-1)^l j^{2l}, \qquad l = 0, \ldots, N, \tag{31}$$

$$B_{lk} = \sum_{j=0}^{M}{}' (-1)^{(k+l)} j^{2(k+l)}, \qquad k, l = 0, \ldots, N. \tag{32}$$

The solution of this system yields the desired coefficients A_k in the local ABC (25)–(26).

It should be remarked that if $N \geq 2$, special finite elements must be used in the layer adjacent to B, which possess high-order regularity. This is necessary due to the high-order derivatives that are involved in the ABC (25)–(26) in this case. A hierarchy of such elements in two and three dimensions has been devised in Givoli and Keller (1994)–Patlashenko and Givoli (1997). However, here we shall take $N = 1$; with this choice standard C^0 finite element may be used throughout. We note that the value of M does *not* affect the regularity of the finite element formulation.

4 Computational Aspects

At time step $n+1$ and at simple-iteration $(i+1)$, the problem to be solved in Ω consists of the nonlinear elliptic equation (14), the boundary conditions (8) and (9) on Γ, and the ABC (25)–(26) on B. This problem is solved by the Galerkin finite element method. Finite element discretization leads to the system of nonlinear algebraic equations

$$K d_{n+1} = F_{n+1}(d_{n+1}) \tag{33}$$

where

$$K = \mathop{A}_{e=1}^{N_{el}} k^e, \qquad F_{n+1} = \mathop{A}_{e=1}^{N_{el}} f_{n+1}^e \tag{34}$$

$$k^e = \bar{k}^e + \tilde{k}^e, \qquad f_{n+1}^e = \bar{f}_{n+1}^e + \tilde{f}_{n+1}^e \tag{35}$$

$$\bar{k}_{ab}^e = \alpha^{-2} \int_{\Omega^e} \nabla N_a \cdot \nabla N_b \, d\Omega + \int_{\Omega^e} N_a N_b \, d\Omega \tag{36}$$

$$\tilde{k}_{ab}^e = \alpha^{-2} \int_{B^e} N_a L_N N_b \, dB = \frac{1}{R\alpha^2} \sum_{m=0}^{N} A_m (-1)^m \int_{B^e} \frac{\partial^m N_a}{\partial \theta^m} \frac{\partial^m N_b}{\partial \theta^m} \, dB \tag{37}$$

$$(\bar{f}_a^e)_{n+1} = \int_{\Omega^e} N_a \tilde{f}(u_{n+1}) \, d\Omega + \int_{\Gamma_h^e} N_a h_{n+1} \, dB - \sum_{b=1}^{N_{en}} (g_b^e)_{n+1} \bar{k}_{ab}^e \tag{38}$$

$$(\tilde{f}_a^e)_{n+1} = \alpha^{-2} \int_{B^e} N_a H[\tilde{f}(u_{n+1}^{(i)})] \, dB \tag{39}$$

In (33), K is the global stiffness matrix, d_{n+1} is the solution vector, and F_{n+1} is the load vector. In (34), N_{el} is the total number of elements and $\mathop{A}_{e=1}^{N_{el}}$ is the assembly operator. In (35), the matrix $\bar{k}^e$ and the vector $\bar{f}_{n+1}^e$ are the standard element stiffness matrix and load vector, whereas $\tilde{k}^e$ and $\tilde{f}_{n+1}^e$ are the contributions due to the ABC (25)–(26) on B. In (36)–(39), a and b are indices corresponding to the element nodes, N_a is the element shape function associated with node a, Ω^e is the domain of element e, and Γ_h^e and B^e are, respectively, the parts of the boundary of element e which are on Γ_h and on B. In (38), N_{en} is number of element nodes, and $(g_b^e)_{n+1}$ is either the value of the function g_{n+1} at node b of element e, if this node is located on Γ_g, and zero otherwise.

Note that we have omitted the index $(i+1)$ from all the variables in (33)–(39) for brevity; however, in (39) we indicate that H is calculated based on u from the previous iteration, i.e., $u_{n+1}^{(i)}$. The nonlinearity of (33) is due to the dependence of the load vector F on the solution vector d, through $\tilde{f}(u_{n+1})$ in (38). The nonlinear algebraic system (33) is solved using Newton iterations. It is easy to show that the tangent stiffness matrix is symmetric in this case: see Givoli and Patlashenko (1998).

The overall solution procedure is similar to the one discussed in Givoli and Patlashenko (1998); the only essential difference

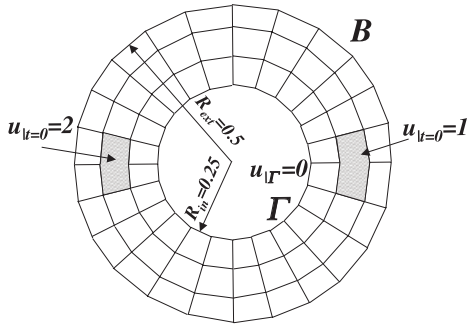

Figure 2 : Setup for the initial pulse problem.

is the new definition of $\tilde{k}^e$ in (37), which is based here on the *local* ABC (25)–(26), and is thus performed on the element level. The solution scheme consists of *three loops*: the time-step loop (indicated by n), the simple-iteration loop (indicated by i), and the Newton-iteration process which is the innermost loop. The convergence criterion for stopping either of the latter two processes is based on evaluating the residual norms and comparing them to some given tolerances.

The computation of $H[\tilde{f}]$ in (24) involves the calculation of the Fourier coefficients of the function $\tilde{f}$ given by (13), for $\xi \geq R$. This is most efficiently done by using the discrete Fast Fourier Transform (FFT). In any event, it is necessary to keep track of $\tilde{u}_{n+1}$, defined by (5), in D. To this end, and for the purpose of performing the integration in (24) and (17), the annular domain $R \leq r \leq r_{\max}$, for some sufficiently large $r_{\max}$, is divided into integration cells with polar geometry. The integrals in (24) and (17) are calculated numerically by using a simple trapezoidal rule per integration-cell in both the r- and θ-directions. For additional details on this integration, see Givoli and Patlashenko (1998).

5 Numerical Experiments

We consider the nonlinear wave equation (1) in the infinite two-dimensional domain exterior to an obstacle with a circular boundary Γ of radius $a = 0.25$. The nonlinear function in (1) is $f(u) = -qu^3$ where $q = 10000$. As shown in Strauss (1989) (see also Givoli and Patlashenko (1998)), for this choice of nonlinear function, a solution exists globally. The obstacle is soft, i.e., $u = 0$ at $r = a$. No sources are present. The wave velocity is $c = 17.5$. The initial rate $\dot{u}$ is zero throughout the domain, whereas the initial value of u is zero except at two small regions, as described in Fig. 2. For the time discretization we employ the Newmark method with parameters $\beta = 0.25$, $\gamma = 0.5$ and with a time-step interval of $\Delta t = 0.005$.

As a reference solution with which all other computed solutions are compared, we numerically construct an "exact" solution, obtained by using a very large domain ($R = 30$), a very fine mesh, and using the DtN condition on B with a large number of terms. (Note, however, that the time-step size Δt remains as above.) All other computations are performed using a circular artificial boundary B of radius $R = 0.5$, and a finite element mesh of bilinear quadrilateral elements in Ω, containing three circumferential layers of elements, with 24 elements in each layer.

On B, we apply either the nonlocal DtN condition (20)–(24), with M terms in the expansions (21) and (24), or the optimal local ABC (25)–(26), of first order ($N = 1$) and with M modes taken in (31) and (32). We note that, as was shown in Givoli and Patlashenko (1998), a "naive" boundary condition on B like the Sommerfeld-like condition yields very poor accuracy, and in fact may alter the qualitative behavior of the numerical solution altogether. On the other hand, the DtN condition, and as we shall see here also its optimal localized version, capture the correct behavior of the solution.

Fig. 3 shows the "exact" solution at five values of time. The graphs show u as a function of the radial location r along the horizontal line ($\phi = 0°$ and $\phi = 180°$). The waves propagating from the initial pulses, the waves reflected from the soft obstacles, and the "wakes" of the waves (which are characteristic of two-dimensional waves only) are all apparent in the plots. Also, by comparing these graphs with those appearing in Patlashenko and Givoli (2000) which correspond to the exact solution of the *linear* problem, one can notice the effects of the nonlinearity. The nonlinearity is responsible for significant changes in the instantaneous amplitude of the wave, although the general form of the waves is retained.

In Fig. 4, the "exact" solution is compared with the computed solution obtained by using the optimal local ABC with $M = N = 1$, along the horizontal line $\phi = 0°$. It is apparent that the simple first-order optimal ABC captures the wave behavior very well. In contrast, the Sommerfeld-like ABC (which is actually a zero-order ABC, and which is not shown in the figure) yields a completely erroneous result and quickly goes beyond the scale of the figure.

We measure $||e||$, the $L_2(B)$ norm of the error $e = u - u^h$, where u is the "exact" solution and u^h is the finite element solution. Tab. 1 summarizes the errors generated by using the nonlocal and local ABCs on B. It gives the values of $\log_{10}||e||^2$ for two time values and various values of M. The nonlocal condition with $M = 20$ yields the smallest error; in fact the error is mainly due to the spatial discretization, since the representation of the far-field behavior is very accurate with this ABC. In contrast, the nonlocal conditions with small M yield a very large error; much larger than the error produced by the optimal local condition with the same M. This phenomenon is related to the well-known fact in the time-harmonic case that for a sufficiently small M the nonlocal DtN condition is unstable due to lack of uniqueness of the problem in Ω on the continuous level (Patlashenko and Givoli (1997); Harari and Hughes (1992)).

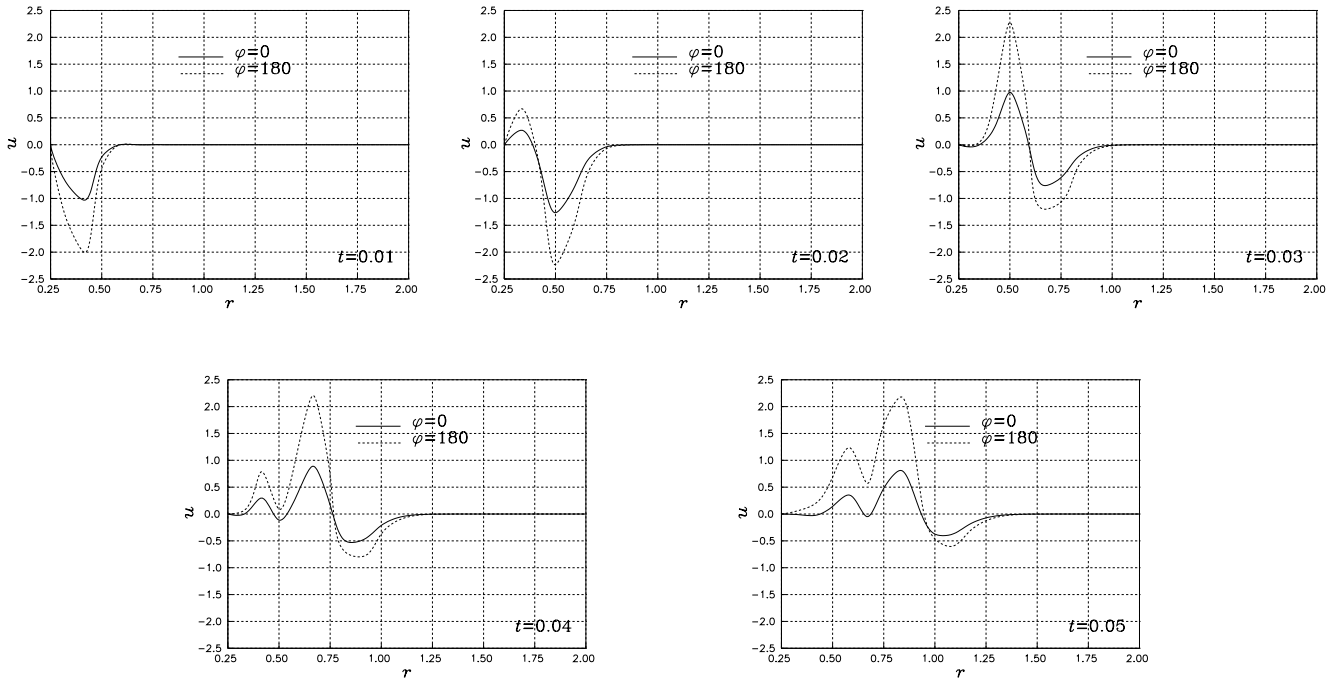

Figure 3 : The initial pulse problem: 'exact' solution at five time values along the horizontal rays $\phi = 0^\circ$ and $\phi = 180^\circ$.

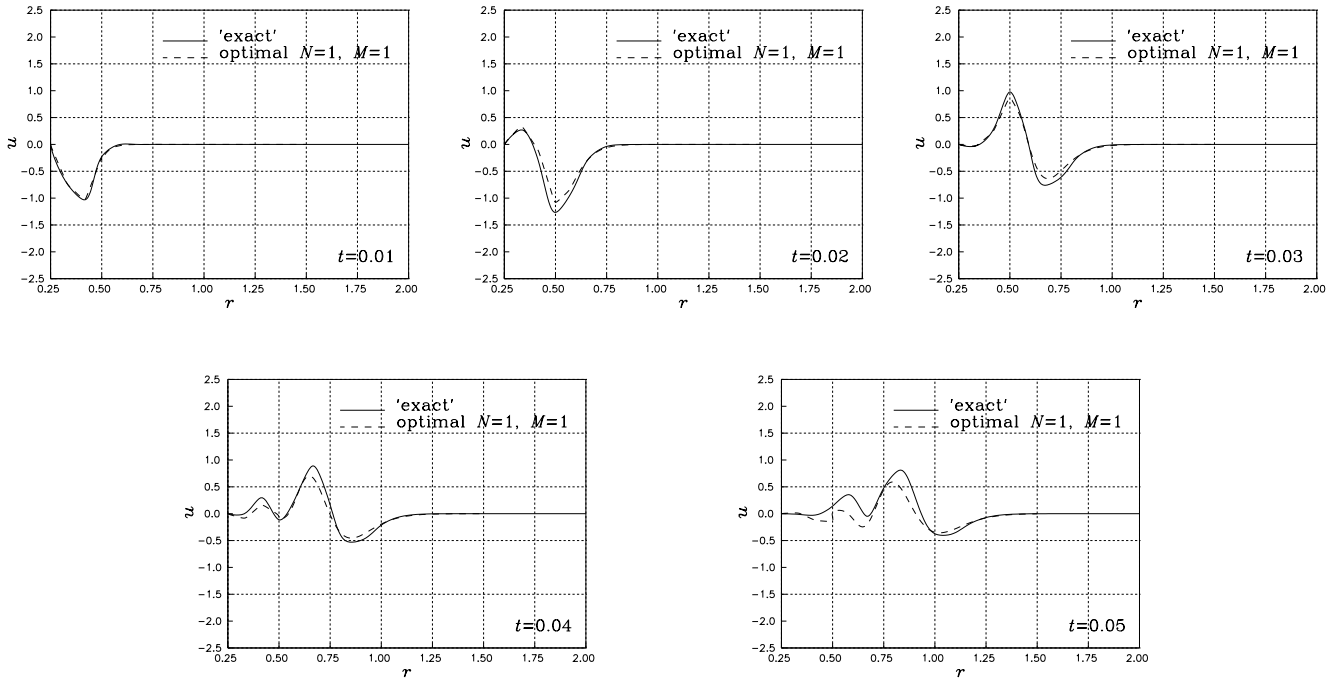

Figure 4 : The initial pulse problem: 'exact' and computed solutions at five time values along the horizontal ray $\phi = 0^\circ$.

Table 1 : Errors ($\log_{10}||e||^2$) generated by using various nonlocal and local ABCs on B.

Nonlocal				
$M=0$	$M=1$	$M=4$	$M=10$	$M=20$
$t=0.01$				
-0.531	-0.535	-0.579	-0.586	-0.598
$t=0.025$				
0.560	0.549	0.208	0.184	0.175
Optimal Local, $N=1$				
$t=0.01$				
-0.595	-0.595	-0.595	-0.595	-0.595
$t=0.025$				
0.182	0.179	0.178	0.188	0.194

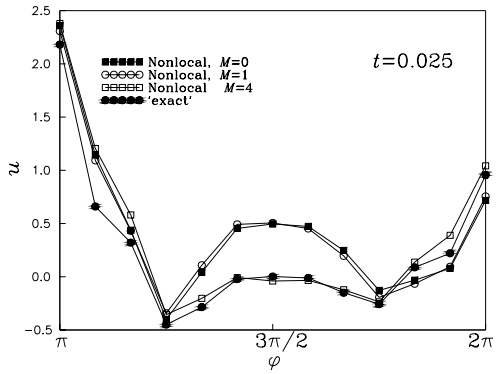

Figure 5 : The initial pulse problem: the solution obtained by using the nonlocal DtN condition on B as a function of the angle ϕ for $t=0.025$ and $r=0.417$.

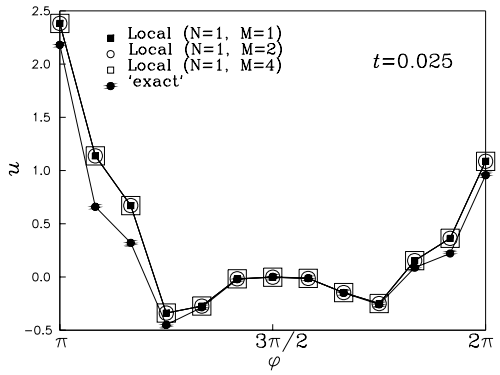

Figure 6 : The initial pulse problem: the solution obtained by using an optimal local ABC on B as a function of the angle ϕ for $t=0.025$ and $r=0.417$.

Another observation from Tab. 1 is that the optimal local ABC performs very well; the errors produced with $M=1$, $M=2$ and $M=4$ are only slightly larger than the error associated with the nonlocal ABC with $M=20$. It is interesting to note that $M=4$ yields the best result, and that the use of a much larger M causes the error to increase. The explanation to this is the following. The local ABCs are optimal in the least-squares sense (i.e., with respect to the L_2 norm), over all the modes from 1 to M. If the Fourier content of the exact solution is such that the first M_0 modes are dominant whereas all modes beyond the M_0 mode are relatively weak, it would be counterproductive to take $M > M_0$, thus "smearing" the error over modes that are not active. In the example considered here there are four major modes, and this explains the results of Tab. 1. Of course, in a complicated problem it is often very difficult to estimate the number of important modes *a priori*. This difficulty may be overcome by using an iterative scheme in which M is modified adaptively based on the computed solution.

Some of these observations may also be seen in Fig. 5 and Fig. 6, where the computed solution is shown at $t=0.025$ and $r=0.417$ as a function of the angle ϕ. In Fig. 5 the result of using three nonlocal ABCs is compared with the "exact" solution, whereas in Fig. 6 three optimal local ABCs are employed. Again it is apparent that the nonlocal ABCs with $M=0$ and $M=1$ are unstable, and that the optimal ABCs with $M=1$, $M=2$ and $M=4$ yield almost the same solution. In both cases, the errors are larger closer to the regions of the initial pulses (the shaded regions in Fig. 2), and are very small away from these regions.

6 Concluding Remarks

In this paper we proposed a finite element scheme for the solution of nonlinear exterior wave problems. The formulation is similar to the one devised in Givoli and Patlashenko (1998), with one major difference: whereas Givoli and Patlashenko (1998) is based on the use of the nonlocal exact DtN boundary condition (20), here we use the local approximate ABC (25)–(26). The latter ABC is obtained by localizing the DtN condition in a systematic way which guarantees a minimal distance (in the L_2 sense) between the actions of the local and nonlocal operators.

We have demonstrated, through numerical experiments, that the replacement of the DtN condition with a low-order "optimal" local ABC is beneficial, in that it yields results which are not significantly less accurate that the DtN results, and at the same time it involves much less computational effort.

One aspect which is worth improving in the present scheme is the need for *integration over a portion of the exterior domain*. An effort to free the numerical scheme from this need is currently underway.

We have concentrated on the relatively simple model of the two-dimensional nonlinear scalar (Klein-Gordon) equation.

However, we believe that the scheme may be extended to more complex nonlinear exterior wave problems, such as problems of large-amplitude water waves and nonlinear elastic waves.

Acknowledgement: This work was partly supported by the U.S.-Israel Binational Science Foundation (BSF), Grant No. 97-00120, and by the Fund for the Promotion of Research at the Technion.

References

Givoli, D. (1991): Non Reflecting Boundary Conditions, *J. Comput. Phys.*, vol. 94, pp. 1–29.

Givoli, D. (1992): *Numerical Methods for Problems in Infinite Domains*, Elsevier, Amsterdam.

Tsynkov, S. V. (1998): Numerical Solution of Problems on Unbounded Domains, A Review, *Appl. Numer. Math.*, vol. 27 , pp. 465–532.

Bayliss A.; Turkel, E. (1980): Radiation Boundary Conditions for Wave-Like Equations, *Comm. Pure Appl. Math.*, vol. 33, pp. 707–725.

Ferm, L.; Gustafsson, B. (1982): A Down-Stream Boundary Procedure for the Euler Equations, *Comp. Fluids*, vol. 10, pp. 261–276.

Engquist, B.; Majda, A. (1981): Numerical Radiation Boundary Conditions for Unsteady Transonic Flow, *J. Comp. Phys.*, vol. 40, pp. 91–103.

Thomas, J.; Salas, M. D. (1986): Far Field Boundary Conditions for Transonic Lifting Solutions to the Euler Equations, *AIAA J.*, vol. 24, pp. 1074–1080.

Hagstrom, T.; Hariharan, S. I. (1988): Accurate Boundary Conditions for Exterior Problems in Gas Dynamics, *Math. Comput.*, vol. 51, pp. 581–97.

Don, W.-S.; Gottlieb, D. (1990): Spectral Simulations of an Unsteady Compressible Flow Past a Circular Cylinder, *Comp. Meth. Appl. Mech. Engng*, vol. 80, pp. 39–58.

Abarbanel, S.; Don, W.-S.; Gottlieb, D.; Rudy, D. H.; Townsend, J. C. (1991): Secondary Frequencies in the Wake of a Circular Cylinder with Vortex Shedding, *J. Fluid Mech.*, vol. 225, pp. 557–574.

Verhoff, A.; Stookesberry, D. (1992): Second-Order Far-Field Computational Boundary Conditions for Inviscid Duct Flow Problems, *AIAA J.*, vol. 30, pp. 1268–1276.

Hagstrom, T. (1991): Conditions at the Downstream Boundary for Simulations of Viscous, Incompressible Flow, *SIAM J. Sci. Stat. Comp.*, 12, pp. 843-858.

Tsynkov, S. V. (1995): An Application of Nonlocal External Conditions to Viscous Flow Computations, *J. Comput. Phys.*, 116, pp. 212–225. 14

Ryaben'kii, V. S.; Tsynkov, S. V. (1995): Artificial Boundary Conditions for the Numerical Solution of External Viscous Flow Problems," *SIAM J. Numer. Anal.,* vol. 32, pp. 1355–1389.

Tsynkov, S. V.; Turkel, E.; Abarbanel, S. (1996): External Flow Computations Using Global Boundary Conditions, *AIAA J.*, vol. 34, pp. 700–706.

Pearson, R. A. (1974): Consistent Boundary Conditions for the Numerical Models of Systems That Admit Dispersive Waves, *J. Atmos. Sci.*, vol. 31, pp. 1418–1489.

Halpern, L.; Schatzman, M. (1989): Artificial Boundary Conditions for Viscous Incompressible Flows, *SIAM J. Math. Anal.*, vol. 20, pp. 308–353.

Jin, G.; Braza, M. (1993): A Nonreflecting Outlet Boundary Condition for Incompressible Unsteady Navier-Stokes Calculations, *J. Comput. Phys.*, vol. 107, pp. 239–253.

Danowitz, J. S.; Abarbanel, S. A. and Turkel, E. (1995): A Far-Field Non-Reflecting Boundary Condition for Two-Dimensional Wake Flows, ICASE Rep. 95-63, NASA Langley, Hampton, VA.

Givoli, D.; Patlashenko, I. (1998): Finite Element Solution of Nonlinear Time-Dependent Exterior Wave Problems, J. Comput. Phys., 143, pp. 241–258, 1998.

Givoli, D. (1999): Recent Advances in the DtN Finite Element Method for Unbounded Domains, *Archives of Comput. Meth. in Engng.*, vol. 6, pp. 71–116.

Givoli, D. (1999): Exact Representations on Artificial Interfaces and Applications in Mechanics, *Appl. Mech. Reviews*, vol. 52, pp. 333–349.

Malhotra, M.; Pinsky, P. M. (1996): Matrix-free interpretation of the non-local Dirichlet-to-Neumann radiation boundary condition, *Int. J. Numer. Meth. Engng.* vol. 39, pp. 3705–3713.

Givoli, D.; Patlashenko, I. (1998): Optimal Local Non-Reflecting Boundary Conditions," Applied Numerical Mathematics, Vol. 27, pp. 367–384, 1998.

Sidi, A.; Givoli, D. (to appear): Stability and Accuracy of Optimal Local Non-Reflecting Boundary Conditions, *Appl. Numer. Math.*.

Patlashenko, I.; Givoli, D. (to appear): Optimal Local Non-Reflecting Boundary Conditions for Time-Dependent Waves, *J. Computational Acoustics*.

Whitham, G. B. (1974): *Linear and Nonlinear Waves*, Wiley, New York.

Wright, T. W.; ed. (1986): *Nonlinear Wave Propagation in Mechanics*, ASME Publications, New York.

Segel, L. A. (1987): *Mathematics Applied to Continuum Mechanics*, Dover, New York.

Strauss, W. A. (1989) *Nonlinear Wave Equations*, American Mathematical Society, Providence, RI.

Givoli, D. (1992): A Spatially Exact Non-Reflecting Boundary Condition for Time Dependent Problems, *Comput. Meth. Appl. Mech. Engng.*, vol. 95, pp. 97–113.

Givoli, D.; Keller, J. B. (1994): Special Finite Elements for use with High-order Boundary Conditions, *Computer Methods in Applied Mechanics and Engineering*, vol. 119, pp. 199–213.

Givoli, D.; Patlashenko, I.; Keller, J. B. (1997): High Order Boundary Conditions and Finite Elements for Infinite Domains, *Comp. Meth. Appl. Mech. Engng.*, vol. 143, pp. 13–39.

Patlashenko, I.; Givoli, D. (1997): Non-Reflecting Finite Element Schemes for Three-Dimensional Acoustic Waves, *J. Comput. Acoustics*, vol. 5, pp. 95–115.

Harari, I.; Hughes, T. J. R. (1992): Analysis of Continuous Formulations Underlying the Computation of Time-harmonic Acoustics in Exterior Domains, *Comput. Meth. Appl. Mech. Engng.*, vol. 97, pp. 103–124.